Reducing Sugar: New Functional Molecules for the Green Synthesis of Graphene Nanosheets

Chengzhou Zhu, Shaojun Guo, Youxing Fang, and Shaojun Dong*

State Key Laboratory of Electroanalytical Chemistry, Changchun Institute of Applied Chemistry, Chinese Academy of Sciences, Changchun 130022, China, and Graduate School of the Chinese Academy of Sciences, Beijing, 100039, China

ABSTRACT In this paper, we developed a green and facile approach to the synthesis of chemically converted graphene nanosheets (GNS) based on reducing sugars, such as glucose, fructose and sucrose using exfoliated graphite oxide (GO) as precursor. The obtained GNS is characterized with atomic force microscopy, UV—visible absorption spectroscopy, transmission electron microscopy, X-ray photoelectron spectroscopy, and so on. The merit of this method is that both the reducing agents themselves and the oxidized products are environmentally friendly. It should be noted that, besides the mild reduction capability to GO, the oxidized products of reducing sugars could also play an important role as a capping reagent in stabilizing as-prepared GNS simultaneously, which exhibited good stability in water. This approach can open up the new possibility for preparing GNS in large-scale production alternatively. Moreover, it is found that GNS-based materials could be of great value for applications in various fields, such as good electrocatalytic activity toward catecholamines (dopamine, epinephrine, and norepinephrine).

KEYWORDS: graphene nanosheets · reducing sugar · electrocatalysis · catecholamines

Two-dimensional graphene nanosheets (GNS) and graphene-based materials have received significant attention in recent years due to their unique electronic, mechanical, and thermal properties since their discovery in 2004.[1,2] This unique nanostructure holds great promise for potential applications in many technological fields such as nanoelectronics,[3] sensors,[4,5] capacitors,[6] and nanocomposites.[7,8] At present, GNS have been prepared by a variety of techniques, including micromechanical cleavage,[1] chemical processing,[9−11] epitaxial growth,[12] and so on. Among these methods, chemical reduction of exfoliated GO is an efficient approach to large-scale production of GNS in low cost, which include noncovalent, covalent functionalization of reduced graphene oxide,[13−16] and so on. It is noted that a key challenge in the synthesis and processing of bulk-quantity GNS is apt to aggregation owing to the strong $\pi-\pi$ stacking tendency between GNS. However, aggregation can be overcome by the attachment of other molecules or polymers onto the nanosheets. For example, polymer-coated "graphitic nanoplatelets" obtained by reducing exfoliated GO in the presence of poly(sodium-4-styrene sulfonate)[17,18] and poly(*N*-vinyl-2-pyrrolidone)[8] were reported. However, the presence of foreign stabilizers is generally undesirable for most applications. On the other hand, the chemical reduction of the GO was usually carried out using hydrazine/hydrazine derivatives as the reducing agent.[19−21] Unfortunately, the use of highly toxic and dangerously unstable hydrazine or dimethylhydrazine to reduce GO requires great care.

Recently, Zhang et al. reported the individual graphene oxide sheets can be readily reduced under a mild condition using L-ascorbic acid.[22] This supplies an environmentally friendly approach for large-scale production of water-soluble graphene. However, lengthy experimental time (48 h) and the limited reducing agent (L-ascorbic acid) constrain its practical application. Therefore, green and facile approaches to the large-scale production of GNS based on a general method remain a great challenge.

Glucose is a mostly studied analyte of great biological importance. It is naturally employed as a reducing agent owing to its mild reductive ability and nontoxic property. To date, investigations into the one-pot synthesis of GNS based on glucose reduction route have not been carried out. In this paper, we demonstrated a green and facile approach to prepare GNS via employing glucose as a reducing agent (Scheme 1). Furthermore, the effect of different various saccharides (fructose and sucrose) on

*Address correspondence to dongsj@ciac.jl.cn.

Received for review February 5, 2010 and accepted March 23, 2010.

Published online April 1, 2010.
10.1021/nn1002387

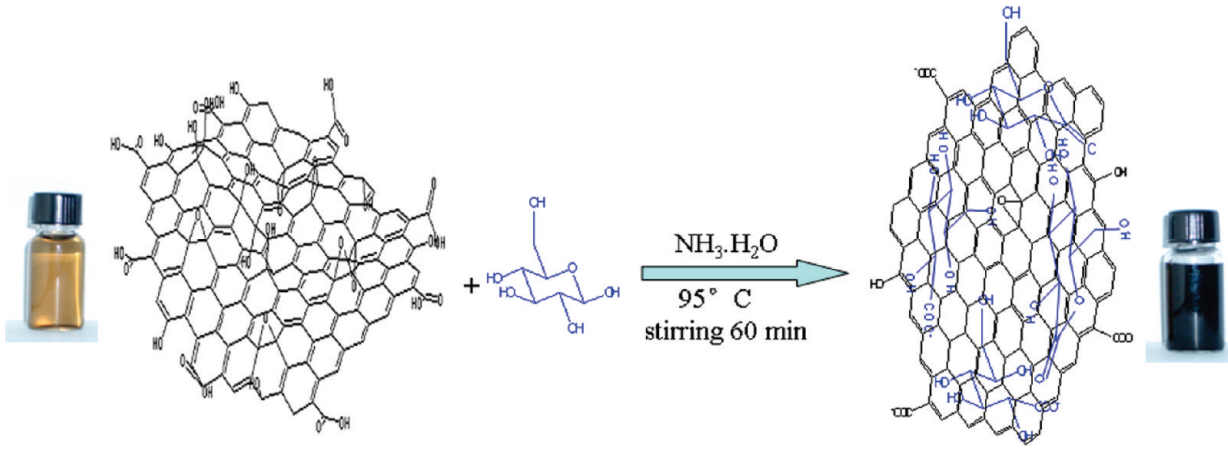

Scheme 1. Illustration of the preparation of GNS based on glucose reduction.

GO reduction was also studied and the similar results were obtained. The merit of this method is that the saccharides themselves and the oxidized products are environmentally friendly. It would be reasonable to expect that besides the mild reduction capability to GO, the oxidized products of glucose may also play an important role as a capping reagent in stabilizing as-prepared GNS simultaneously. Most important, electrochemical behaviors of catecholamines compounds (dopamine, epinephrine, and norepinephrine) were studied, which showed remarkably strong and stable electrocatalytic response.

RESULTS AND DISCUSSION

A one-pot method for water-phase synthesis of GNS based on glucose reduction was demonstrated. Briefly, the dispersion of GO in water was first prepared from graphite by modified Hummers method.[23] Then, glucose was added into the aqueous dispersion of GO with ammonia solution. It was found that GO could be rapidly reduced in the presence of both glucose and ammonia. As a comparison, in a control experiment, the reduction rate of GO was slow in the absence of ammonia solution. Moreover, we found that GO was also partially reduced only in the presence of ammonia solution while keeping other conditions unchanged. Therefore, the introduction of the ammonia solution provided a synergistic augmentation of the reaction rate and was favorable to deoxygenation of GO. This result was consistent with the work reported previously.[24] The reduction of GO was first monitored by time-dependent UV−vis spectroscopy. As shown in Figure 1A, the UV−vis absorption peak of the GO dispersion at 230 nm gradually red shift to 261 nm and the absorption in the whole spectral region increases with reaction time, suggesting that GO is reduced and the electronic conjugation within the graphene sheets is restored upon glucose reduction. Little increase in absorption was found after 60 min when the mixture was stirred for 60 min at 95 °C. Hence, the reaction time was fixed to 60 min for later experiment. The reduction of GO is also indicated from the color change of the solution before and after reaction (from brown to dark, as shown in Figure 1B (vials a,b). The obtained GNS could be stably dispersed in water for more than one month. In the meantime, it was found that GO can also be reduced partially at room temperature due to the weak reduction capability. Figure 1B (vial c) shows the

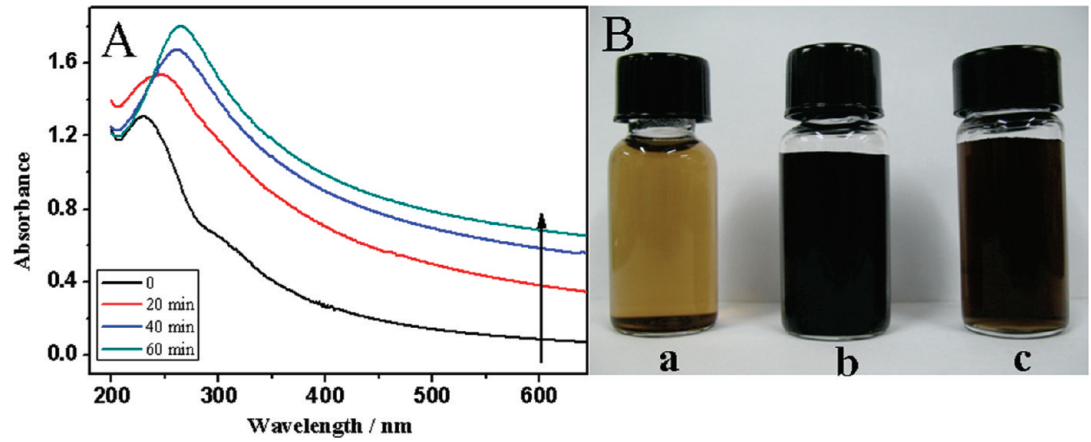

Figure 1. (A) UV−vis absorption spectra showing the change of GO dispersions as a function of reaction time. (B) Photographs of aqueous dispersions (0.1 mg/mL) of GO before (a) and after (b, c) the reduction with glucose, which were kept at 95 °C for 60 min (b) and at room temperature over 48 h (c).

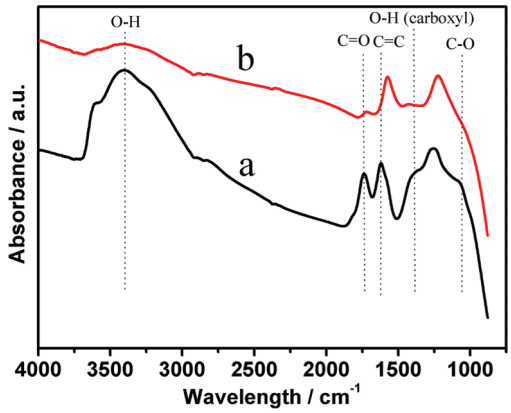

Figure 2. FTIR spectra of GO (a) and the obtained GNS (b).

photographs of the obtained GNS in water at room temperature when reaction time was fixed to 48 h. Obviously, the elevated temperature can efficiently accelerate the reaction rate. The reduction of the oxygen-containing groups in GO by glucose was also confirmed by FTIR spectroscopy (Figure 2). The FTIR spectra of GO (Figure 2a) shows a strong absorption band at 1739 cm^{-1} due to the C═O stretching. The spectrum of GO also exhibits the presence of O−H (ν_{O-H} at 3403 and 1395 cm^{-1}), C═C ($\nu_{C=C}$ at 1619 cm^{-1}), and C−O (ν_{C-O} at 1060 cm^{-1}).[25,26] As shown in Figure 2b, after the GO is chemically reduced, the characteristic absorption bands of oxide groups (ν_{O-H}, $\nu_{C=O}$, and ν_{C-O}) decreased dramatically, indicating that such GO has been reduced to the GNS.

Figure 3 is a typical AFM image of GO and GNS dispersion (Figure 3A,C) in water after their deposition on a freshly cleaved mica surface through a drop-casting method. It is clear that similar to the original GO dispersion, the as-prepared GNS remain separated in the dispersion. The average thickness of as-prepared GNS, measured from the height profile of the AFM image (Figure 3D), is about 1.1 nm. Compared with the well-exfoliated GO sheets, with a thickness of about 0.97 nm, the thickness of GNS is larger (Figure 3B). It is reasonable to conclude that the capping reagent play an important role in increasing the thickness of the as-prepared GNS, though most of the oxygen-containing functional groups were removed after the reduction.

Figure 4 shows the TEM images of the large GNS obtained by glucose reduction at different magnifications. There are some corrugations and scrollings on the edge of the graphene, which is consistent with previous works.[27,28] Furthermore, the selected area electron diffraction (SAED) of GNS, as shown in the inset in Figure 4B, suggests that the graphene has good crystalline characteristic.

To further illustrate the formation of graphene, XPS was performed to characterize the removal of the oxygen groups. Figure 5A shows the C1s deconvolution spectrum of GO. Four different peaks centered at 284.5,

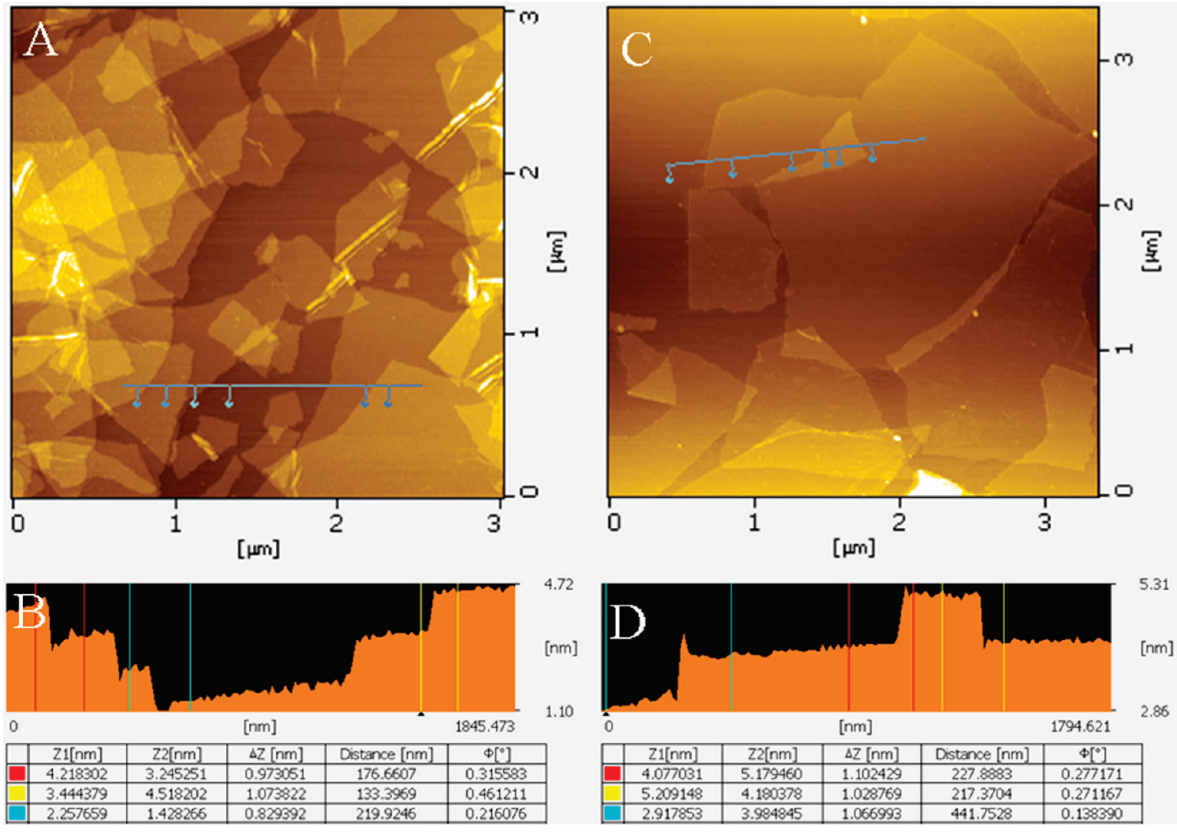

	Z1[nm]	Z2[nm]	ΔZ [nm]	Distance [nm]	Φ[°]
	4.218302	3.245251	0.973051	176.6607	0.315583
	3.444379	4.518202	1.073822	133.3969	0.461211
	2.257659	1.428266	0.829392	219.9246	0.216076

	Z1[nm]	Z2[nm]	ΔZ [nm]	Distance [nm]	Φ[°]
	4.077031	5.179460	1.102429	227.8883	0.277171
	5.209148	4.180378	1.028769	217.3704	0.271167
	2.917853	3.984845	1.066993	441.7528	0.138390

Figure 3. AFM images (A, C) and height profiles (B, D) along the lines shown in AFM images of exfoliated GO (A, B) and as-prepared GNS (C, D) based on glucose reduction in water (0.1 mg/mL) on freshly cleaved mica surface through drop-casting method.

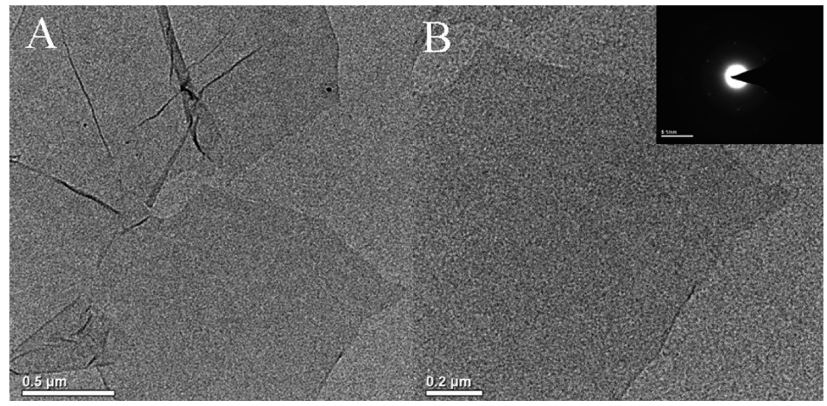

Figure 4. Typical TEM images of the as-synthesized GNS at different magnifications. The inset in (B) is the SAED of GNS.

285.6, 286.6, and 288.4 eV are observed, corresponding to C═C/C−C in aromatic rings, C−OH, C (epoxy and alkoxy), and C═O groups, respectively. For GNS (Figure 5B), the intensities of all C1s peaks of the carbon binding to oxygen, especially the peak of C−O (epoxy and alkoxy), decreased dramatically, indicating that most of the oxygen-containing functional groups were removed after the reduction.

Raman spectroscopy is one of the most widely used techniques to characterize the structural and electronic properties of graphene including disorder and defect structures, defect density, and doping levels. In many cases, the Raman spectrum of graphene is characterized by two main features, the G mode arising from the first order scattering of the E_{2g} phonon of sp^2 C atoms (usually observed at ~1575 cm^{-1}) and the D mode arising from a breathing mode of κ-point photons of A_{1g} symmetry (~1350 cm^{-1}). Herein, as shown in Figure 6A (trace a), the Raman spectrum of the graphite shows the in-phase vibration of the graphite lattice at 1577 cm^{-1} (G band) and a weak D band at 1354 cm^{-1}.[29] In the Raman spectrum of GO (Figure 6A, trace b), the G band is broadened and blue shifts to 1581 cm^{-1} due to the presence of isolated double bonds that resonate at higher frequencies than the G band of graphite.[30] In addition, the D band at 1353 cm^{-1} becomes prominent, indicating the reduction in size of the in-plane sp^2 domains due to the extensive oxidation. After its reduction with glucose, the Raman spectrum of as-prepared GNS also exhibits the presence of D and G bands at 1354 and 1584 cm^{-1}, respectively (Figure 6A, trace c). It should be noted that the frequency of the G and D bands in the GNS are very similar to that observed in the GO. However, the increase in the D/G intensity ratio, compared to pristine graphite, indicates a decrease in the size of the in-plane sp^2 domains and a partially ordered crystal structure of the GNS.[31]

At the same time, we further characterized the crystal structure of GNS by XRD. Figure 6B shows the XRD patterns of the pristine graphite, GO, and GNS. Compared with the pristine graphite (Figure 6B, trace a), the feature diffraction peak of exfoliated GO appears at 10.4° (002) is observed with interlay space (*d*-spacing) of 0.76 nm (Figure 6B, trace b). This value is larger than the *d*-spacing (0.34 nm) of pristine graphite ($2\theta = 26.5°$), as a result of the introduction of oxygenated functional groups on carbon sheets. For the resulting GNS (Figure 6B, trace c), the peak located at 10.4° disappeared, confirming the great reduction of GO and the exfoliation of the layered GNS.[10,32,33]

We have also examined the thermal stability of the prepared GNS and compared it with that of pristine graphite and GO using TGA. As shown in Figure 7c, the GO exhibits about 7 wt % loss below 100 °C and more

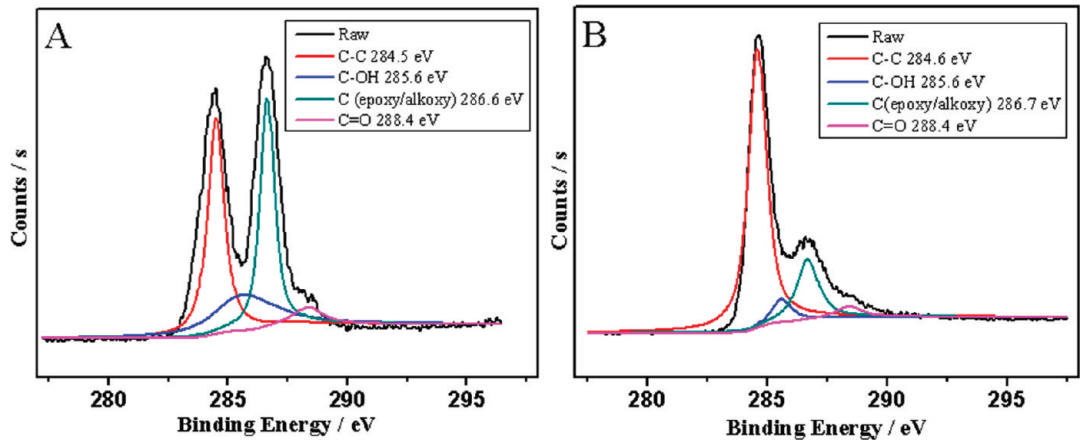

Figure 5. The C1s XPS spectra of (A) GO and (B) GNS.

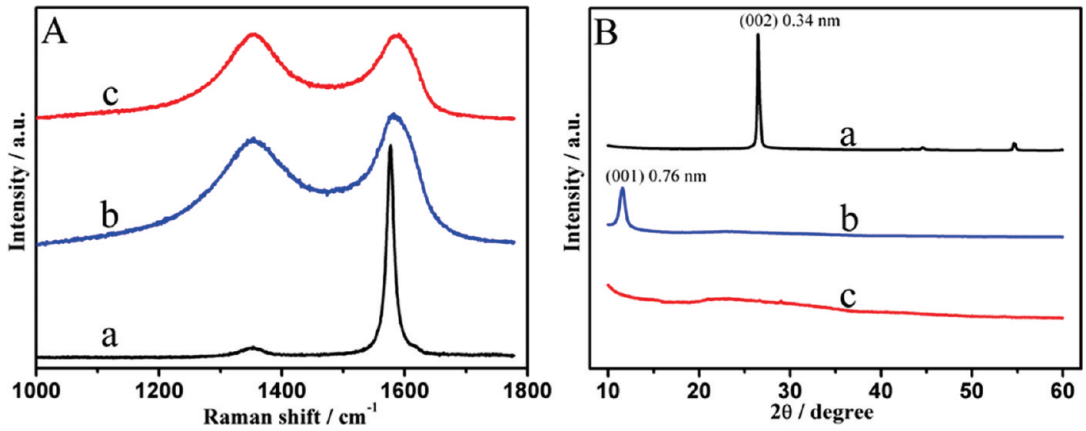

Figure 6. Raman spectra (A) and XRD patterns (B) of pristine graphite (a), GO (b), and GNS (c) after its reduction with glucose.

than 22 wt % loss at 200 °C, resulting from the removal of the labile oxygen-containing functional groups such as CO, CO_2, and H_2O vapors. In contrast, the removal of the thermally labile oxygen functional groups by chemical reduction increased the thermal stability of graphene. It was shown a 4 wt % loss in a nitrogen atmosphere at 200 °C for the GNS (Figure 7b), which was much lower than that of the GO, indicating a decreased amount of oxygenated functional groups. A significant drop of GNS in mass around 600 °C is due to the bulk pyrolysis of carbon skeleton, which is similar to graphite and GO.

Electrochemical impedance spectroscopy (EIS) is the most decisive and directive parameter to reflect the changes of conducting features of electrode/electrolyte interface.[25,34] The Nyquist plot of EIS measurement shows a semicircle in the high-frequency region associated with resistance and capacitance elements in parallel while it shows a straight line in the low-frequency region associated with mass transfer. R_{et} represents electron-transfer resistance and can be accurately read out in the parameters obtained from the fit of the equivalent circuit. As shown in Figure 8c, when exfoliated GO is modified onto a glassy carbon electrode (GCE) surface, the semicircle dramatically increases as compared to the bare GCE, suggesting that

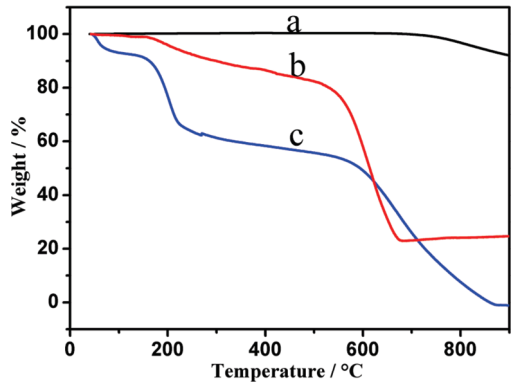

Figure 7. TGA curves of graphite (a), GNS (b), and GO (c).

the attachment of exfoliated GO to the electrode may play a blocking effect and inhibit the rate of charge transfer due to its bad conductivity and repellency between the surface charges of the exfoliated GO and ferricyanide/ferrocyanide ions. After the exfoliated GO is reduced with glucose, the semicircles decrease distinctively, indicating that GNS has accelerated electron transfer between the electrochemical probe $[Fe(CN)_6]^{3-/4-}$ and the electrode, whereas the electron-transfer resistance is still bigger than that of bare GCE (Figure 8a,b).

The reduction of GO using glucose provides a green and facile method to produce high-quality GNS. Motivated by the consideration as to whether other saccharides, such as D-fructose and sucrose, has a similar effect on the GNS synthesis under the same condition. Figure 9 shows the photographs of aqueous dispersions of GO before (a) and after the reduction with fructose (b) and sucrose (c). As is expected, the same results were obtained. In other words, these saccharides can not only act as the efficient reducing agents, but also play an important role in stabilizing as-prepared GNS simultaneously. Moreover, we studied the synthetic mechanism with respect to the saccharide reduction. As an aldohexose, glucose was oxidized to aldonic acid by GO in the presence of ammonia solution. The aldonic acid can further be converted into lactone. Thus, the oxidized products could contain a large number of hydroxyl groups and carboxyl groups. In addition, the reduced GO may have some residual oxygen functionalities, such as the periphery carboxylic groups mentioned above. Thus, hydroxyl group and carboxyl group containing in the oxidized products of glucose might form hydrogen bonds with the residual oxygen functionalities on the reduced GO surfaces. Also of note, excess glucose could contribute to the stabilization of the obtained GNS. Moreover, the electrostatic repulsion induced by the residual oxygen functionalities on the reduced GO surfaces also played an important role in stabilizing GNS. Such interactions can disrupt the

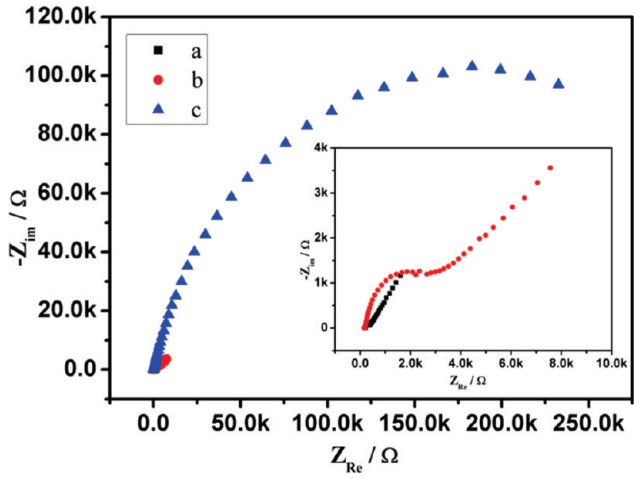

Figure 8. Nyquist plot for the Faradaic impedance measurements in the solution containing 2.5 mM $K_3[Fe(CN)_6]/K_4[Fe(CN)_6]$ (1:1) as redox probe and 0.1 M KCl as supporting electrolyte: (a) bare GCE, (b) GNS-modified GCE, and (c) GO-modified GCE.

$\pi-\pi$ stacking interaction between the reduced GO sheets and further prevent the formation of the agglomerates. As is known, fructose can readily transform into reducing sugar because ketoenol tautomerism occurs in the presence of base (ammonia solution), even though it is classified as a nonreducing sugar. As to sucrose, an important disaccharide, hydrolysis breaks the glycosidic bond, converting sucrose into glucose and fructose. These monosaccharides could contribute to the reduction of GO. Compared with the glucose and fructose, though the same reaction condition is carried out, the reduction capability of sucrose is weaker. This result can be found from the color change before and after reaction with different reducing agents. Therefore, this green and facile approach based on this general method could open up the new possibility for preparing GNS in large-scale production alternatively.

We compared the CVs obtained for $K_3Fe(CN)_6/K_4Fe(CN)_6$ at GNS/GCE, GO/GCE, and bare GCE (Figure 10A). As we can see from Figure 10A (trace a), no obvious redox peaks were observed on GO modified GCE, suggesting that $Fe(CN)_6^{4-/3-}$ redox couple has a very slow electron transfer kinetics, possibly due to the presence of negatively charged oxygen containing moieties of GO and the poor conductivity of the exfoliated GO. After the exfoliated GO was chemically reduced by glucose, a pair of redox wave was obtained (Figure 10A, trace b), although the peak current obtained was smaller than that obtained at bare GCE under the same experimental conditions (Figure 10A, trace c). And CV measurements agree quite well with the EIS experiment mentioned above.

Figure 9. Photographs of aqueous dispersions (0.1 mg/mL) of GO before (a) and after the reduction with fructose (b) and sucrose (c) under the same reaction condition as with glucose.

It is well known that the most abundant catecholamines are epinephrine, norepinephrine, and dopamine, which act as neuromodulators in nervous system or as hormones in the blood circulation. Because of their electrochemical activities, their detection is always attracting an intense interest in electroanalysis.[35−37] The utilization of the obtained GNS modified electrode for electrocatalysis of catecholamines (dopamine, epinephrine, and norepinephrine) was demonstrated. Figure 10B−D shows CVs obtained at bare GCE (a), GO/GCE (b), and GNS/GCE (c) in 0.1 M phosphate buffer solution (PBS, pH = 7.4) containing 1 mM dopamine (B), 1 mM adrenaline (C), and 0.025 mM norepinephrine (D). The larger current densities are achieved at GNS/GCE than those of GO/GCE and bare GCE, suggesting that the GNS exhibited better electrochemical activity than those of the bare GCE and GO/GCE. It should be noted that the current density achieved at GO/GCE observed from CVs suggests that the GO exhibited good enrichment for the analytes in spite of its bad conductivity. We speculate that the difference in current density obtained at GNS/GCE or bare GCE depends on the capability of accumulation for various analytes. Thus, the improved electrochemical response obtained at GNS/GCE can be ascribed to the following three aspects: (1) the as-prepared GNS has the good conductivity and abound surface area; (2) the $\pi-\pi$ interaction between analytes and basal planes of graphene also plays an important role in electrocatalysis oxidation; (3) it was postulated that the better electrochemical activity observed herein might also be due to the hydrogen bonding interaction between analytes and hydroxyl group and carboxyl group contained in the capping reagent or the residual oxygen functionalities on the reduced GO surfaces, which further accelerate the accumulation of the catecholamines; (4) besides, electrostatic interaction between the resulting GNS and target molecules in neutral pH solution should play an important role in enhancing electrochemical response. Based on the higher electrocatalytic activities to the compounds mentioned above, GNS obtained via glucose reduction may be a good material for con-

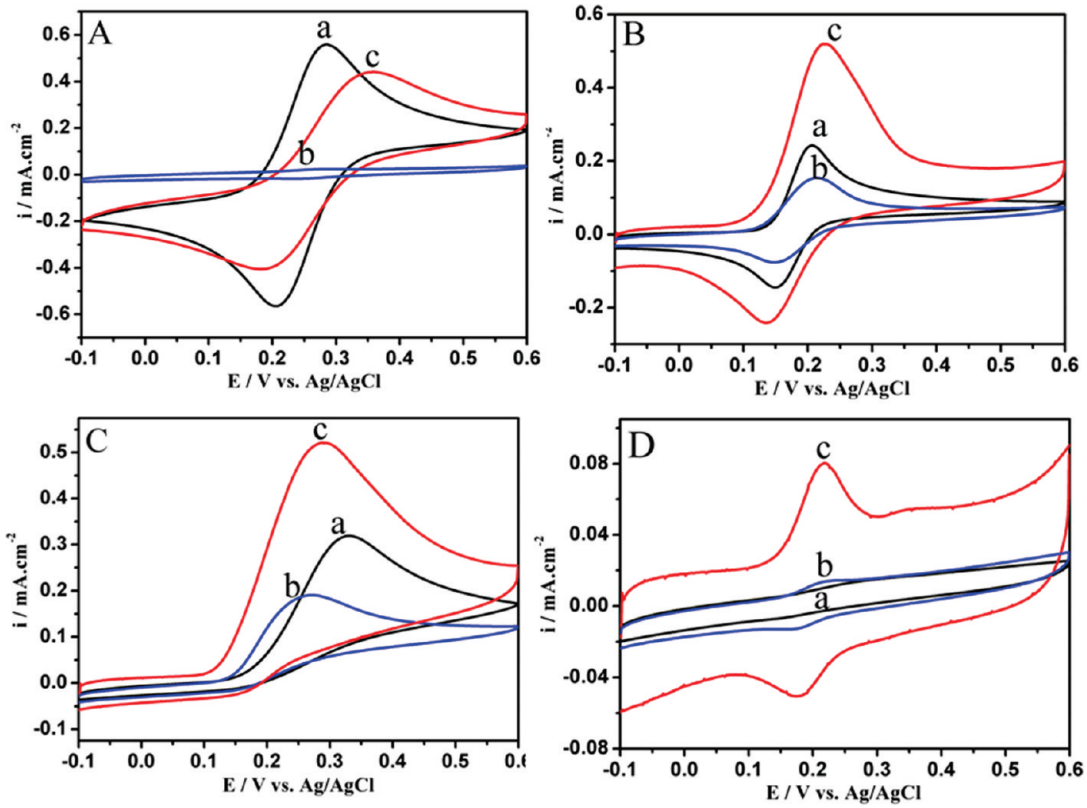

Figure 10. Cyclic voltammograms (CVs) obtained at bare GCE (a), GO/GCE (b), and GNS/GCE (c) in 0.10 M KCl solution containing 2.5 mM $K_3Fe(CN)_6$ and 2.5 mM $K_4Fe(CN)_6$ (A) and in 0.1 M PBS (pH = 7.4) containing 1 mM DA (B), 1 mM adrenaline (C), and 0.025 mM noradrenalin (D). Scan rate: 50 mV/s.

structing a novel and promising electrochemical sensing platform for detecting other biomolecules.

CONCLUSION

In summary, a green and facile approach to the synthesis of GNS based on reducing sugar is reported using exfoliated GO as precursor. The merit of this method is that the glucose itself and the oxidized products are environmentally friendly. It should be noted that, besides the mild reduction capability to GO, the oxidized products of glucose could also play an important role as the capping reagent in stabilizing as-prepared GNS simultaneously. Furthermore, a variety of saccharides, such as glucose, fructose, and sucrose were successfully demonstrated to reduce the exfoliated GO. The obtained GNS could be stably dispersed in water for more than one month. This simple approach should find practical applications in large-scale production of water-soluble GNS. Moreover, GNS-based materials show the good electrocatalytic activity toward catecholamines (dopamine, epinephrine, and norepinephrine).

EXPERIMENTAL SECTION

Chemicals. Graphite was purchased from Alfa Aesar. Glucose, D-fructose, and sucrose were obtained from Beijing Chemical Factory (Beijing, China) and used as received without further purification. Unless otherwise stated, other reagents were of analytical grade and were used as received. All aqueous solutions were prepared with ultrapure water (>18 MΩ) from a Milli-Q Plus system (Millipore).

Apparatus. AFM was conducted with a SPI3800N microscope (Seiko Instruments, Inc.). Infrared spectra were collected on a VERTEX 70 Fourier transform infrared (FTIR) spectrometer (Bruker). UV−vis detection was carried out on a Cary 50 UV−vis-NIR spectrophotometer (Varian, U.S.A.). TEM images were obtained with a TECNAI G2 high-resolution transmission electron microscope operating at 200 kV. Thermogravimetric analyze (TGA) of sample was performed on a Pyris Diamond TG/DTA Thermogravimetric Analyzer (Perkin-Elmer Thermal Analysis). Sample was heated under nitrogen atmosphere from room temperature to 900 at 5 °C min^{-1}. Raman spectra were obtained on a J-Y T64000 Raman spectrometer with 514.5 nm wavelength incident laser light. X-ray diffraction (XRD) spectra were obtained using a D8 ADVANCE (Germany) using Cu Kα (1.5406 Å) radiation. X-ray photoelectron spectroscopy (XPS) analysis was carried on an ESCALAB MK II X-ray photoelectron spectrometer. The electrochemical impedance (EIS) experiments were performed in the presence of 2.5 mM $K_3[Fe(CN)_6]/K_4[Fe(CN)_6]$ (1:1) as the redox probe. The spectra were measured by Autolab with PGSTAT 30 (Eco Chemie B.V., Utrecht, Netherlands) and with the aid of a frequency response analysis system software under an oscillation potential of 5 mV over a frequency range of 100 kHz to 0.01 Hz. Cyclic voltammetry (CV) experiments were performed with a CHI 832 electrochemical analyzer (CH Instruments, Chenhua Co., Shanghai, China). A conventional three-electrode cell was used, including an Ag/AgCl (saturated KCl) electrode as reference electrode, a platinum wire as counterelectrode, and the bare and modified glassy carbon electrode (GCE) as working electrode.

Preparation of GO. The graphite oxide was synthesized from natural graphite powder based on a modified Hummers method.[23] Then, exfoliation of graphite oxide to GO was achieved by ultrasonication of the dispersion for 40 min (1000 W, 20% amplitude). Finally, a homogeneous GO aqueous dispersion (0.5 mg/mL) was obtained and used for further characterizations and the chemical reduction.

Preparation of the GNS Based on Glucose Reduction. In a typical procedure for chemical conversion of graphene oxide to GNS, 40 mg glucose was added into 25 mL of homogeneous GO dispersion (0.1 mg/mL), followed by stirring for more than 0.5 h. Then, to the resulting dispersion were added 20 μL of ammonia solution (25% w/w). After being vigorously shaken or stirred for a few minutes, the mixture was stirred for 60 min at 95 °C. Finally, the resulting stable black dispersion was centrifuged (15000 rpm) and washed with water for three times. Then, the obtained GNS was redispersed in water before further use. The procedure to the preparation of GNS based on D-fructose and sucrose was the same as mentioned above, except adding D-fructose and sucrose instead of glucose.

Electrochemical Measurements. GCE (3 mm in diameter) was polished with 1.0 and 0.3 μm alumina slurry sequentially and then washed ultrasonically in water and ethanol for a few minutes, respectively. The cleaned GCE was dried with a high-purify nitrogen steam for the next modification. A total of 5 μL of GNS or graphene oxide suspension (0.2 mg/mL) was dropped on the pretreated GCE surface and dried at room temperature to form GNS-modified GCE.

Acknowledgment. This research was supported by the National Natural Science Foundation of China (Nos. 20935003 and 20820102037) and 973 Project (Nos. 2009CB930100 and 2010CB933600).

REFERENCES AND NOTES

1. Novoselov, K. S.; Geim, A. K.; Morozov, S. V.; Jiang, D.; Zhang, Y.; Dubonos, S. V.; Grigorieva, I. V.; Firsov, A. A. Electric field effect in atomically thin carbon films. *Science* **2004**, *306*, 666–669.
2. Novoselov, K. S.; Jiang, D.; Schedin, F.; Booth, T. J.; Khotkevich, V. V.; Morozov, S. V.; Geim, A. K. Two-dimensional atomic crystals. *Proc. Natl. Acad. Sci. U.S.A.* **2005**, *102*, 10451–10453.
3. Sui, Y.; Appenzeller, J. Screening and interlayer coupling in multilayer graphene field-effect transistors. *Nano Lett.* **2009**, *9*, 2973–2977.
4. Zhou, M.; Zhai, Y. M.; Dong, S. J. Electrochemical sensing and biosensing platform based on chemically reduced graphene oxide. *Anal. Chem.* **2009**, *81*, 5603–5613.
5. Shan, C. S.; Yang, H. F.; Song, J. F.; Han, D. X.; Ivaska, A.; Niu, L. Direct electrochemistry of glucose oxidase and biosensing for glucose based on graphene. *Anal. Chem.* **2009**, *81*, 2378–2382.
6. Wang, Y.; Shi, Z. Q.; Huang, Y.; Ma, Y. F.; Wang, C. Y.; Chen, M. M.; Chen, Y. S. Supercapacitor devices based on graphene materials. *J. Phys. Chem. C* **2009**, *113*, 13103–13107.
7. Cao, A. N.; Liu, Z.; Chu, S. S.; Wu, M. H.; Ye, Z. M.; Cai, Z. W.; Chang, Y. L.; Wang, S. F.; Gong, Q. H.; Liu, Y. F. A facile one-step method to produce graphene-CdS quantum dot nanocomposites as promising optoelectronic materials. *Adv. Mater.* **2010**, *22*, 103–106.
8. Guo, S. J.; Dong, S. J.; Wang, E. K. Three-dimensional Pt-on-Pd bimetallic nanodendrites supported on graphene nanosheet: Facile synthesis and used as an advanced nanoelectrocatalyst for methanol oxidation. *ACS Nano* **2010**, *4*, 547–555.
9. Wang, H. L.; Robinson, J. T.; Li, X. L.; Dai, H. J. Solvothermal reduction of chemically exfoliated graphene sheets. *J. Am. Chem. Soc.* **2009**, *131*, 9910–9911.
10. Yang, H. F.; Shan, C. S.; Li, F. H.; Han, D. X.; Zhang, Q. X.; Niu, L. Covalent functionalization of polydisperse chemically-converted graphene sheets with amine-terminated ionic liquid. *Chem. Commun.* **2009**, 3880–3882.
11. Park, S.; An, J. H.; Piner, R. D.; Jung, I.; Yang, D. X.; Velamakanni, A.; Nguyen, S. T.; Ruoff, R. S. Aqueous suspension and characterization of chemically modified graphene sheets. *Chem. Mater.* **2008**, *20*, 6592–6594.
12. Berger, C.; Song, Z. M.; Li, T. B.; Li, X. B.; Ogbazghi, A. Y.; Feng, R.; Dai, Z. T.; Marchenkov, A. N.; Conrad, E. H.; First, P. N.; de Heer, W. A. Ultrathin epitaxial graphite: 2D electron gas properties and a route toward graphene-based nanoelectronics. *J. Phys. Chem. B* **2004**, *108*, 19912–19916.
13. Xu, Y. F.; Liu, Z. B.; Zhang, X. L.; Wang, Y.; Tian, J. G.; Huang, Y.; Ma, Y. F.; Zhang, X. Y.; Chen, Y. S. A graphene hybrid material covalently functionalized with porphyrin: Synthesis and optical limiting property. *Adv. Mater.* **2009**, *21*, 1275–1279.
14. Bai, H.; Xu, Y. X.; Zhao, L.; Li, C.; Shi, G. Q. Non-covalent functionalization of graphene sheets by sulfonated polyaniline. *Chem. Commun.* **2009**, 1667–1669.
15. Shen, J. F.; Hu, Y. Z.; Li, C.; Qin, C.; Shi, M.; Ye, M. X. Layer-by-layer self-assembly of graphene nanoplatelets. *Langmuir* **2009**, *25*, 6122–6128.
16. Hao, R.; Qian, W.; Zhang, L. H.; Hou, Y. L. Aqueous dispersions of TCNQ-anion-stabilized graphene sheets. *Chem. Commun.* **2008**, 6576–6578.
17. Stankovich, S.; Dikin, D. A.; Dommett, G. H. B.; Kohlhaas, K. M.; Zimney, E. J.; Stach, E. A.; Piner, R. D.; Nguyen, S. T.; Ruoff, R. S. Graphene-based composite materials. *Nature* **2006**, *442*, 282–286.
18. Wang, G. X.; Shen, X. P.; Wang, B.; Yao, J.; Park, J. Synthesis and characterisation of hydrophilic and organophilic graphene nanosheets. *Carbon* **2009**, *47*, 1359–1364.
19. Tung, V. C.; Allen, M. J.; Yang, Y.; Kaner, R. B. High-throughput solution processing of large-scale graphene. *Nat. Nanotechnol.* **2009**, *4*, 25–29.
20. Stankovich, S.; Dikin, D. A.; Piner, R. D.; Kohlhaas, K. A.; Kleinhammes, A.; Jia, Y.; Wu, Y.; Nguyen, S. T.; Ruoff, R. S. Synthesis of graphene-based nanosheets via chemical reduction of exfoliated graphite oxide. *Carbon* **2007**, *45*, 1558–1565.
21. Stankovich, S.; Piner, R. D.; Chen, X. Q.; Wu, N. Q.; Nguyen, S. T.; Ruoff, R. S. Stable aqueous dispersions of graphitic nanoplatelets via the reduction of exfoliated graphite oxide in the presence of poly(sodium 4-styrenesulfonate). *J. Mater. Chem.* **2006**, *16*, 155–158.
22. Zhang, J. L.; Yang, H. J.; Shen, G. X.; Cheng, P.; Zhang, J. Y.; Guo, S. W. Reduction of graphene oxide via L-ascorbic acid. *Chem. Commun.* **2010**, *46*, 1112–1114.
23. Li, Y. G.; Wu, Y. Y. Coassembly of graphene oxide and nanowires for large-area nanowire alignment. *J. Am. Chem. Soc.* **2009**, *131*, 5851–5857.
24. Fan, X. B.; Peng, W. C.; Li, Y.; Li, X. Y.; Wang, S. L.; Zhang, G. L.; Zhang, F. B. Deoxygenation of exfoliated graphite oxide under alkaline conditions: A green route to graphene preparation. *Adv. Mater.* **2008**, *20*, 4490–4493.
25. Guo, H. L.; Wang, X. F.; Qian, Q. Y.; Wang, F. B.; Xia, X. H. A green approach to the synthesis of graphene nanosheets. *ACS Nano* **2009**, *3*, 2653–2659.
26. Shan, C. S.; Yang, H. F.; Han, D. X.; Zhang, Q. X.; Ivaska, A.; Niu, L. Water-soluble graphene covalently functionalized by biocompatible poly-L-lysine. *Langmuir* **2009**, *25*, 12030–12033.
27. Shao, Y. Y.; Wang, J.; Engelhard, M.; Wang, C. M.; Lin, Y. H. Facile and controllable electrochemical reduction of graphene oxide and its applications. *J. Mater. Chem.* **2010**, *20*, 743–748.
28. Si, Y. C.; Samulski, E. T. Synthesis of water soluble graphene. *Nano Lett.* **2008**, *8*, 1679–1682.
29. Tuinstra, F.; Koenig, J. L. Raman spectrum of graphite. *J. Chem. Phys.* **1970**, *53*, 1126–1130.
30. Kudin, K. N.; Ozbas, B.; Schniepp, H. C.; Prud'homme, R. K.; Aksay, I. A.; Car, R. Raman spectra of graphite oxide and functionalized graphene sheets. *Nano Lett.* **2007**, *8*, 36–41.
31. Ferrari, A. C.; Robertson, J. Interpretation of Raman spectra of disordered and amorphous carbon. *Phys. Rev. B* **2000**, *61*, 14095–14107.

32. Hassan, H. M. A.; Abdelsayed, V.; Khder, A.; AbouZeid, K. M.; Terner, J.; El-Shall, M. S.; Al-Resayes, S. I.; El-Azhary, A. A. Microwave synthesis of graphene sheets supporting metal nanocrystals in aqueous and organic media. *J. Mater. Chem.* **2009**, *19*, 3832–3837.
33. McAllister, M. J.; Li, J.-L.; Adamson, D. H.; Schniepp, H. C.; Abdala, A. A.; Liu, J.; Herrera-Alonso, M.; Milius, D. L.; Car, R.; Prud'homme, R. K.; Aksay, I. A. Single sheet functionalized graphene by oxidation and thermal expansion of graphite. *Chem. Mater.* **2007**, *19*, 4396–4404.
34. Xu, D. K.; Xu, D. W.; Yu, X. B.; Liu, Z. H.; He, W.; Ma, Z. Q. Label-free electrochemical detection for aptamer-based array electrodes. *Anal. Chem.* **2005**, *77*, 5107–5113.
35. Wang, Y.; Li, Y. M.; Tang, L. H.; Lu, J.; Li, J. H. Application of graphene-modified electrode for selective detection of dopamine. *Electrochem. Commun.* **2009**, *11*, 889–892.
36. Zhou, M.; Shang, L.; Li, B. L.; Huang, L. J.; Dong, S. J. The characteristics of highly ordered mesoporous carbons as electrode material for electrochemical sensing as compared with carbon nanotubes. *Electrochem. Commun.* **2008**, *10*, 859–863.
37. Wang, L.; Bai, J. Y.; Huang, P. F.; Wang, H. J.; Zhang, L. Y.; Zhao, Y. Q. Self-assembly of gold nanoparticles for the voltammetric sensing of epinephrine. *Electrochem. Commun.* **2006**, *8*, 1035–1040.